https://doi.org/10.1088/1402-4896/ac169c

# LIBS applicability for investigation of re-deposition and fuel retention in tungsten coatings exposed to pure and nitrogen-mixed deuterium plasmas of Magnum-PSI

I. Jõgi[1,*], P. Paris[1], K. Piip[1], J. Ristkok[1], R. Talviste[1], H-M. Piirsoo[1], A. Tamm[1], E. Grigore[2], A. Hakola[3], B. Tyburska-Pueschel[4] and H.J. van der Meiden[4]

[1] *Institute of Physics, University of Tartu, W. Ostwaldi str. 1, 50411 Tartu, Estonia*

[2] *National Institute for Laser, Plasma and Radiation Physics, Euratom-MedC Association, 409 Atomistilor, 077125 Bucharest, Romania*

[3] *VTT Technical Research Centre of Finland Ltd., 02044 VTT, Finland*

[4] *DIFFER - Dutch Institute for Fundamental Energy Research, De Zaale 20, 5612 AJ Eindhoven, the Netherlands*

## Abstract

We have investigated the applicability of Laser Induced Breakdown Spectroscopy (LIBS) for analyzing the changes in the composition and fuel retention of W and W-Ta coatings following exposure to $D_2$ or mixed $D_2$-$N_2$ plasma beams in the linear plasma device Magnum PSI. The exposed samples were characterized by in-situ ns-LIBS and complementary analysis methods Secondary Ion Mass Spectroscopy, Energy Dispersive X-Ray spectroscopy and Nuclear Reaction Analysis. In agreement with the used complementary analysis methods, LIBS revealed the formation of up to 200 nm thick co-deposited surface layer in the central region of the coatings which contained a higher concentration of the main plasma impurities, such as N, and metals, such as Ta and Mo, the latter originating mainly from the substrate and from the plasma source. The deuterium retention on the other hand was highest outside from the central region of the coatings.

*Keywords*: LIBS analysis of ITER relevant tungsten coatings; deuterium plasma exposure; fuel retention; re-deposition

# 1. Introduction

Fuel retention in tokamak walls is a potential safety issue which requires the development of remote composition analysis methods such as Laser Induced Breakdown Spectroscopy (LIBS) [1,2]. LIBS method uses short laser pulses to ablate and ionize tiny amounts of material from the surfaces. The formed plasma plume emits light characteristic for the elemental composition of the ablated material. The composition as well as mechanical and thermal properties of the investigated surface layer influence the properties of the LIBS plasma plume and its emission spectra [3–6]. This means that quantitative determination of the elemental composition and fuel retention from the emission spectra requires additional effort. To this end, it is possible to apply either calibration-free LIBS (CF-LIBS) [7,8] or construct a large database from well-characterized reference samples [2]. CF-LIBS requires that the plasma is both temporally and spatially in local thermodynamic equilibrium which is complicated to be achieved for light elements such as hydrogen isotopes [8,9]. The construction of a LIBS calibration database, on the other hand, requires the comparison of selected spectral lines with the concentrations determined by complementary quantitative analysis methods. In this regard, Nuclear Reaction Analysis (NRA) is often used method for quantitative analysis of fuel retention because it allows both the determination of total amount of retained fuel and its depth profile and [10].

The plasma exposure may further change the composition and mechanical properties of the investigated components due to the modifications of the exposed surface or the formation of co-deposited layers. These changes in material properties may in turn influence the fuel retention and recorded LIBS spectra. The effect of the plasma exposure on the surface properties depends on the composition of the plasma impacting the surfaces [11–13]. Elements such as N or Ne will be used as seeding gases to reduce heat fluxes towards ITER and DEMO divertor surfaces. Regardless of the used gases, they will alter the material morphology and also influence retention characteristics [14]. In addition, nitrogen further forms chemical bonds with tungsten [15,16] and the formed nitride acts as a diffusion barrier which traps the hydrogen isotopes and increases the fuel retention [14,17,18].

We have investigated the applicability of LIBS for analysing the changes in composition and fuel retention of W and W-Ta coatings following exposure to $D_2$ or mixed $D_2$-$N_2$ plasma beams in Magnum PSI linear plasma generator. The samples were subsequently characterized by in-situ ns-LIBS and complementary ex-situ measurements methods to investigate the composition and surface morphology of the exposed coatings.

# 2. Methods

The investigated samples were either 5 µm thick W prepared by DC magnetron sputtering [19] or 7 µm thick W-Ta layers prepared by DC magnetron sputtering and High-power Impulse Magnetron Sputtering (HiPIMS) on 30 mm diameter Mo substrates. The coatings were exposed to $D_2$ or mixed $D_2$-$N_2$(4%) or $D_2$-$N_2$(6%) plasma beams in Magnum PSI for 3000 s. The used $N_2$ percentages were comparable with the percentages used in previous studies where the effect of $N_2$ seeding on deuterium retention was investigated [16–18]. The magnetic field in the Magnum-PSI was 1.2 T and the target voltage -40 V. With the help of Thomson Scattering, the electron temperature was determined to be 1.5-1.6 eV and the electron density 4-5×$10^{19}$ $cm^{-3}$. The plasma flux was 2-4·$10^{23}$ $m^{-2}s^{-1}$, which was somewhat smaller than the fluxes expected in the ITER divertor ($10^{24}$ $m^{-2}s^{-1}$). The full width at half maximum (FWHM) of the plasma beam was 17-18 mm. An example of the distribution of the electron density of the Magnum-PSI plasma beam is shown in figure 1. The surface temperature of samples during the exposure was measured by IR camera (Fig. 1). The temperature was kept within 320-370°C to avoid extensive fuel desorption [20]. The surface temperature was somewhat lower in the outer zone of the plasma beam (Fig. 1).

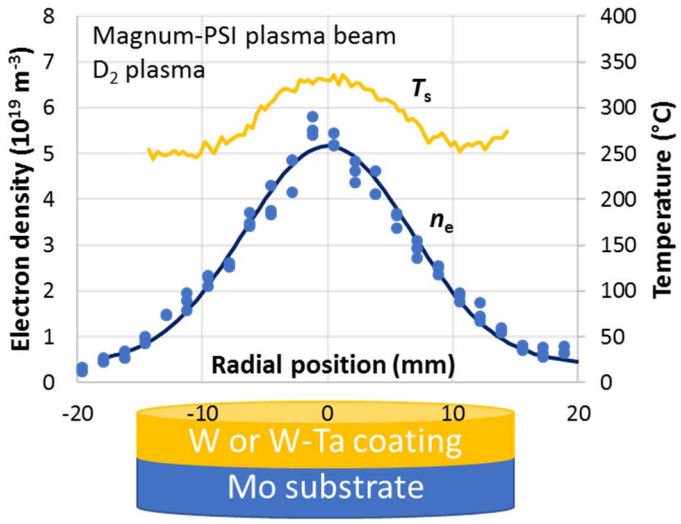


Figure 1. Spatial distribution of the electron density of Magnum-PSI plasma beam and surface temperature during W-Ta exposure to $D_2$ plasma beam.

The samples were subsequently characterized by in-situ ns-LIBS [21,22] in the Target Exchange and Analysis Chamber at 1 mbar of Ar. For the analyses, we used a Nd:YAG laser working at 1064 nm and with a pulse length of 8 ns and fluence of 20 J/$cm^2$ per pulse. The LIBS plasma plume emission was collected and imaged with a magnification of 1 onto a 0.8 mm fibre by a 30 cm focal length lens. The fibre directed the light to a Czerny-Turner spectrometer which was equipped with an Andor iStar camera. The spectrometer registered a 20 nm wide spectral window around the 656.28 nm $H_\alpha$ and 656.10 nm $D_\alpha$

line. The delay of the detection window between the laser pulse and recording of the spectra of the emitted plasma plume was 1300 ns and the gate width was set to 2000 ns. Our previous experience has shown that these values allow to distinguish the peaks of hydrogen isotope while obtaining sufficiently strong signal.

Complementary ex-situ measurements of the coating composition after the plasma exposure were carried out by Scanning Electron Microscopy (SEM), Energy Dispersive X-ray spectroscopy (EDX), Secondary Ion Mass Spectroscopy (SIMS) and NRA. SEM images were used to investigate the surface morphology along the coating surface. EDX was used to investigate the spatial distribution of elemental composition along the surface but it lacks the depth resolution and sensitivity for small concentrations. The depth profiles of selected elements of the original sample or of the co-deposit formed on (D, H, W, Mo, Ta) were investigated by SIMS while the total D retention in the coating was determined by NRA with the probing depth of 3 μm. Glow-Discharge Optical Emission Spectroscopy (GDOES) was used to determine the composition and thickness of the unexposed coatings.

## 3. Results and discussion

Figure 2 shows the appearance of ~1 cm wide dark ring on the coatings following the exposure to the $D_2$–$N_2$(6%) plasma beam. Such rings were observed also on the coatings exposed to pure $D_2$ plasma beam but were less distinct and somewhat narrower (not shown). In the case of exposure of W coating to $D_2$–$N_2$(6%) plasma beam, the central region became also somewhat darker (Fig. 2). The appearance of such rings has been noted also in previous studies and has been attributed to the erosion of the coating subjected to the outer zone of the plasma beam and redeposition on the coating subjected to the inner zone of the plasma beam [12,13]. In this central region of the coating surrounded by the dark ring, the SEM images showed notable changes in surface morphology. In the case of central region of W coating, there appeared large features with the size of hundreds of nanometres attributable to the expected formation of a co-deposit. In the case of the W-Ta coating, the surface of central region was covered with small grains with the size below 100 nm. Outside from this region, the surface of both coatings remained similar to that of unexposed coatings with the appearance of small debris.

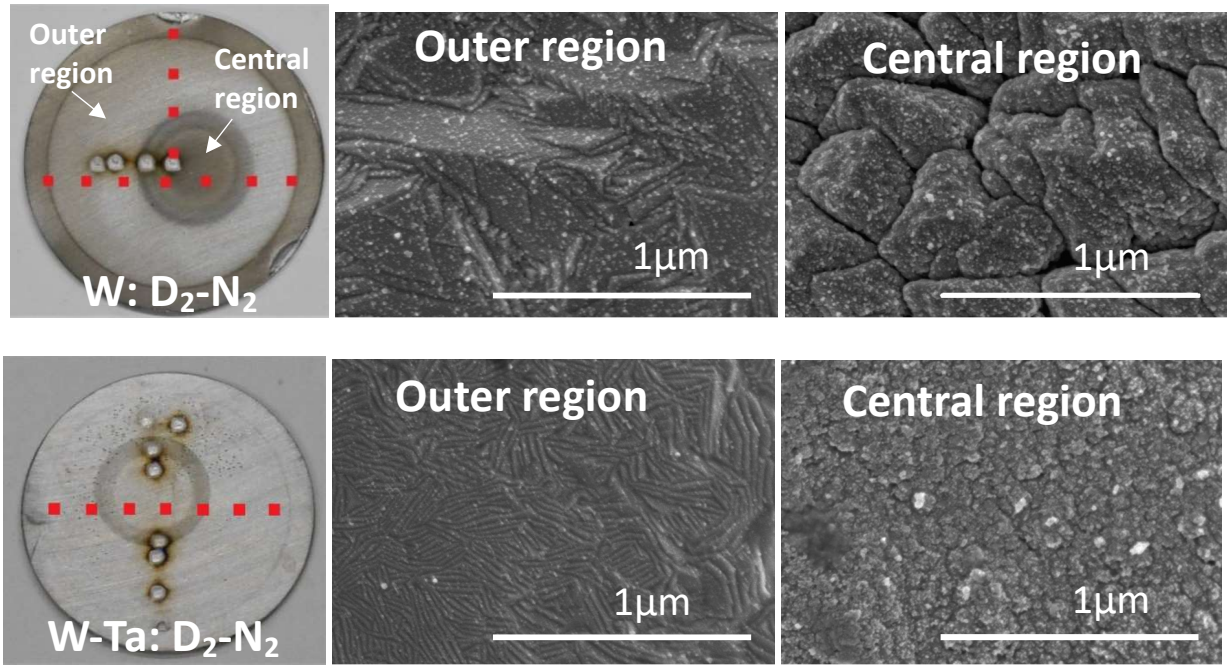


Figure 2. Photos of W and W-Ta sample surfaces and SEM images extracted from the outer and central regions of the coatings exposed to a $D_2$-$N_2$(6%) plasma beam. The light, large spots correspond to the laser craters while the red squares show the measurement regions of NRA.

SEM/EDX results presented in Table 1 show that the exposure of the coatings to $N_2$ containing plasma beam resulted in the appearance of elemental N in the coating. The concentration of N was considerably higher in the coating region exposed to the central zone of the plasma beam. This central region contained also increased concentration of Ta and Mo after the plasma exposure. The increased concentrations of Ta and Mo in the central zone are explainable by the re-deposition on the coating surface exposed to the central zone of plasma beam. Additional Ta may originate from the sputtering of the clamping material while Mo is most likely originating from the electrodes of the plasma source or to some extent from the substrate.

Table 1. EDX determined composition of W and W-Ta layers after the exposure to $D_2$ or $D_2$-$N_2$(6%) plasma beam. The concentrations are shown in at. % and the standard deviation of measurements was 0.5-1 at. %.

| **W: $D_2$** | **W** | **Ta** | **Mo** | **O** | **N** | **W: $D_2$-$N_2$** | **W** | **Ta** | **Mo** | **O** | **N** |
|---|---|---|---|---|---|---|---|---|---|---|---|
| Central region | 81 | 1 | | 18 | | Central region | 57 | 7 | 7 | 15 | 14 |
| Outer region | 93 | | | 7 | | Outer region | 67 | | 1 | 25 | 7 |
| **W-Ta: $D_2$** | **W** | **Ta** | **Mo** | **O** | **N** | **W-Ta: $D_2$-$N_2$** | **W** | **Ta** | **Mo** | **O** | **N** |

| | | | | | | | | | | |
|---|---|---|---|---|---|---|---|---|---|---|
| Central region | 81 | 9 | 2 | 8 | Central region | 43 | 8 | 7 | 21 | 21 |
| Outer region | 87 | 6 | | 7 | Outer region | 54 | 3 | 1 | 35 | 7 |

SIMS depth profiles revealed that the increased amount of N, Ta and Mo in the coating region exposed to the central zone of the plasma beam occurred in a surface layer with a thickness up to 400 nm in the case of $D_2$-$N_2$(6%) plasma exposure (Fig. 3). This is consistent with the proposed co-deposition of Ta and Mo on the central region of coating surface. The deposition of metals such as Ta and Mo on the central region of coating exposed to $D_2$-$N_2$ plasma beam may also cause co-deposition of N atoms from the plasma beam which could explain higher N concentration in the surface layer of this region [18]. The formation of the deposited layer is consistent with the changed appearance of the surface of the central region as seen in SEM images (Fig. 2). The concentration of D was also the highest in this upper layer of the coating, but the distribution was different from those of the other elements. Typically, D signal could be measured only at a very thin surface layer while in some cases, the D signal peaked deeper in the layer deposited during the plasma exposure (Fig. 3). The peak may correspond to the D implantation or is occurring during the early stages of the plasma exposure.

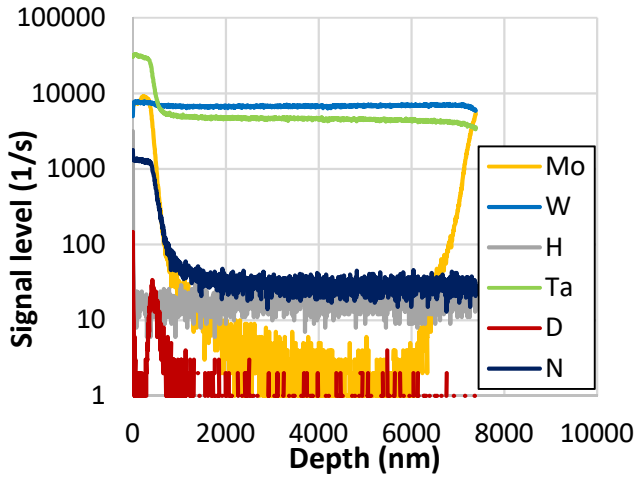


Figure 3. SIMS elemental depth profiles of the W-Ta coating exposed to $D_2$-$N_2$(6%) plasma beam.

An example of LIBS spectra collected during the 3rd shot of a W-Ta coating exposed to outer zone of $D_2$-$N_2$(6%) plasma is shown in figure 4a. The used delay time of 1300 ns was sufficiently long to reduce the Stark broadening of the $D_\alpha$ and $H_\alpha$ lines at 656.10 nm and 656.28 nm and allowed clear separation of these lines. It should be noted that the intensities of $D_\alpha$ and $H_\alpha$ lines were considerably stronger and broader during the 1st shot while the spectra obtained during the 3rd shot was more representative for the bulk of the coating (see also figure 4b). The $D_\alpha$ and $H_\alpha$ line intensities were obtained by fitting the lines

by Lorentz profiles. The presence of a W line at 656.32 nm was also considered during the fitting. The lines of W, Ta and Mo were fitted by Gaussian profiles with a FWHM value of 0.05 nm (apparatus function of the spectrometer).

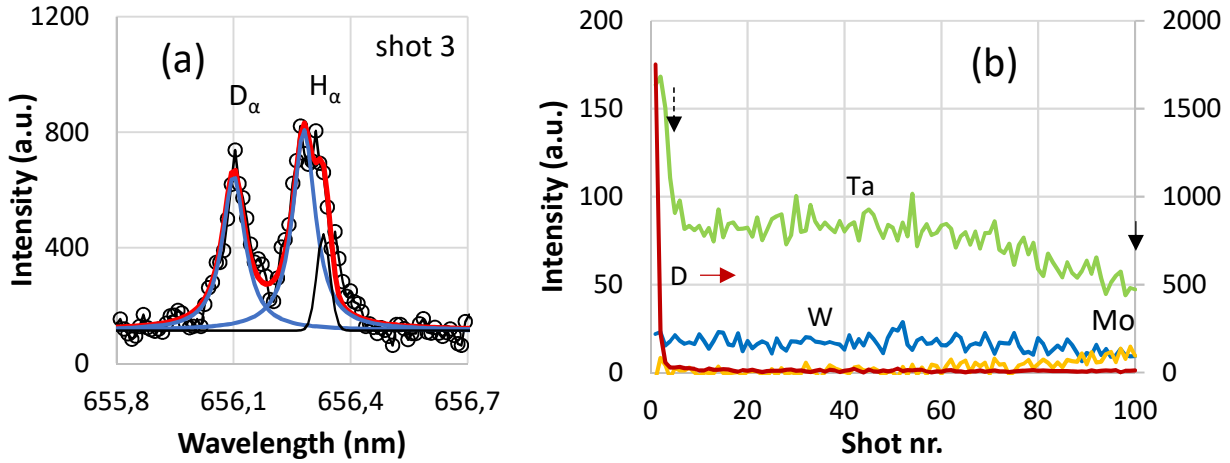


Figure 4. (a) - fitting of the emission spectrum of $D_\alpha$ and $H_\alpha$ lines and (b) LIBS depth profiles of $D_\alpha$, W, Ta and Mo lines of W-Ta coating exposed to a $D_2$-$N_2$(6%) plasma beam.

The depth profiles of the $D_\alpha$ 656.10 nm, W 653.24 nm, Ta 648.54 nm and Mo 651.98 nm lines for a W-Ta coating exposed to a $D_2$-$N_2$ plasma beam are shown in figure 4b. The depth profile of N lines could not be presented because sufficiently strong N lines were missing in the investigated wavelength range between 640-660 nm. The $D_\alpha$ line intensity was the highest on the coating surface and then decreased to a relatively low level which depended on the position along the coating (described in Fig. 5a). Ta and W showed similar profiles after the first 3-4 laser shots. In the investigated wavelength region, the strongest Ta line at 648.54 nm was 4-5 times more intense than the most prominent W line at 653.24 nm even though the Ta concentration was only 6 at. %. The intensity of the Ta line was considerably higher for the first few laser shots in the central region of the W-Ta coatings. This increase was most notable for coatings exposed to $D_2$-$N_2$ plasma beam which is consistent with the SIMS results (Fig. 3).

The average LIBS ablation rate was determined by dividing the coating thickness by the shot number where the W or Ta line intensity decreased to 50% of the signal in the coating (shown by black arrow in the depth profile). The ablation rate depended on the coating composition and was 60 nm/shot for W and 70-80 nm/shot for W-Ta coatings. The ablation rate of the Ta rich surface layer in coating region exposed to central zone of plasma beam was determined on the basis of the LIBS Ta signal (dashed black arrow in Fig. 4b) and the SIMS depth profiles. The ablation rate of this layer was considerably higher, up to 200 nm/shot.

Depth averaged LIBS D line intensity values divided by the W line intensity (D/W line ratio) were obtained by averaging between shot numbers 10-30 for the different spots on the W-Ta coatings. The depth averaged D/W line ratios in different regions of the coatings are shown in figure 5a together with the depth averaged D concentration obtained by NRA. In general, the deuterium concentration was lower inside the central region of the coating contrary to the concentrations of N and Ta. The decrease of D retention may be caused by the higher temperature in the central region of the coating (Fig. 1). Alternatively, it may be caused by differences in the ion and electron power densities delivered to the different sample regions [23]. The D ion flux is distributed relatively smoothly along the entire sample surface while the electron flux and heat flux are distributed more narrowly, being the highest at the centre of the plasma beam.

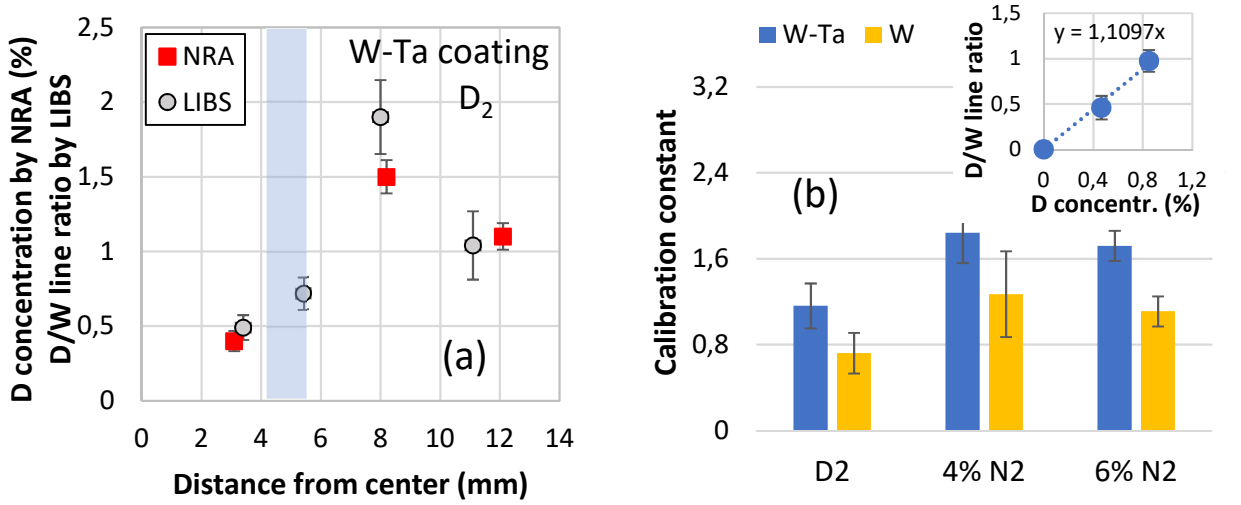


Figure 5. (a) Depth averaged D/W ratio determined by LIBS and depth averaged D concentration determined by NRA as a function of distance from the center of the central dark ring (figure 1) for W-Ta coating exposed to a $D_2$ plasma beam, (b) calibration constants for D/W line ratios determined by LIBS and D concentrations determined by NRA. Inset of figure 5b shows the D/W line ratio determined by LIBS as a function of D concentration determined by NRA in a W-Ta coating exposed to a $D_2$ plasma beam.

A calibration constant for the D/W intensity ratio dependence from the D concentration as determined by NRA was estimated by further averaging the previously calculated D/W ratio and comparing them to the determined D concentrations on the central and outer regions. The dependence and linear fit is shown in the inset of figure 5b for W-Ta coatings exposed to $D_2$ plasma beam. The slope of the linear fit can be considered as a calibration constant which increased in the presence of nitrogen. The slopes were 0.7, 1.3

and 1.1 for W coatings exposed to $D_2$, $D_2$-$N_2$ (4%) and $D_2$-$N_2$(6%) plasma beam, respectively. For W-Ta coatings the corresponding values were 1.1, 1.8 and 1.7. These results reinforce the requirement for extensive calibration of LIBS D/W line ratio for various types of layers.

## 6. Conclusions

The following main results were obtained in the study:

- In the sample region subjected to the central zone of the plasma beam, co-deposited layers containing high amounts of N, Ta and Mo could be found. The thickness of this layer reached up to 400 nm in coatings exposed to the mixed $D_2$-$N_2$ plasma beam.
- D intensity recorded by LIBS agreed with D signal obtained by SIMS and D concentrations determined by NRA. The D signal was highest on the surface layer and decreased deeper in the coating. In the latter part of the coating, the concentration of D was lower in the sample region exposed to the central zone of the plasma beam.
- The relation between the D signal determined by LIBS and the D concentrations by NRA depended on the coating composition and the used gas composition during plasma exposure. For the same D concentration (NRA), the LIBS signal was higher in W-Ta coatings and coatings exposed to $N_2$ containing plasma beams.
- The ablation rate of the coatings was around 60-80 nm/shot and somewhat higher for W-Ta coatings. The ablation rate of the Ta and N rich surface layer reached 200 nm/shot. The presence of layers with very different ablation rates requires careful consideration in the proper quantification of fuel retention.

The results demonstrate the usefulness of LIBS in the remote composition and fuel retention analysis in plasma-facing materials and the impact of the material properties on the LIBS performance.

## Acknowledgements

This work has been carried out within the framework of the EUROfusion Consortium and has received funding from the Euratom research and training programme 2014-2018 and 2019-2020 under grant agreement number 633053. The views and opinions expressed herein do not necessarily reflect those of the European Commission. Present study was partially funded by the European Regional Development Fund project „Emerging orders in quantum and nanomaterials“ (TK134).

## References


[1] Philipps V, Malaquias A, Hakola A, Karhunen J, Maddaluno G, Almaviva S, Caneve L, Colao F, Fortuna E, Gasior P, Kubkowska M, Czarnecka A, Laan M, Lissovski A, Paris P, van der Meiden H J, Petersson P, Rubel M, Huber A, Zlobinski M, Schweer B, Gierse N, Xiao Q and Sergienko G 2013 Development of laser-based techniques for in situ characterization of the first wall in ITER and future fusion devices *Nucl. Fusion* **53** 093002

[2] Malaquias A, Philipps V, Huber A, Hakola A, Likonen J, Kolehmainen J, Tervakangas S, Aints M, Paris P, Laan M, Lissovski A, Almaviva S, Caneve L, Colao F, Maddaluno G, Kubkowska M, Gasior P, Van Der Meiden H J, Lof A R, Zeijlmans Van Emmichoven P A, Petersson P, Rubel M, Fortuna E and Xiao Q 2013 Development of ITER relevant laser techniques for deposited layer characterisation and tritium inventory *J. Nucl. Mater.* **438** S936–9

[3] Laan M, Hakola A, Paris P, Piip K, Aints M, Jõgi I, Kozlova J, Mändar H, Lungu C, Porosnicu C, Grigore E, Ruset C, Kolehmainen J and Tervakangas S 2017 Dependence of LIBS spectra on the surface composition and morphology of W/Al coatings *Fusion Eng. Des.* **121**

[4] Suchonova M, Veis P, Karhunen J, Paris P, Pribula M, Piip K, Laan M, Porosnicu C, Lungu C and Hakola A 2017 Determination of deuterium depth profiles in fusion-relevant wall materials by nanosecond LIBS *Nucl. Mater. Energy* **12** 611–6

[5] Sattar H, Jielin S, Ran H, Imran M, Ding W, Gupta P Das and Ding H 2020 Impact of microstructural properties on hardness of tungsten heavy alloy evaluated by stand-off LIBS after PSI plasma irradiation *J. Nucl. Mater.* **540** 152389

[6] Sattar H, Ran H, Ding W, Imran M, Amir M and Ding H 2020 An approach of stand-off measuring hardness of tungsten heavy alloys using LIBS *Appl. Phys. B Lasers Opt.* **126** 1–11

[7] Ciucci A, Palleschi V, Rastelli S, Salvetti A, Singh D P and Tognoni E 1999 CF-LIPS: A new approach to LIPS spectra analysis *Laser Part. Beams* **17** 793–7

[8] Tognoni E, Cristoforetti G, Legnaioli S and Palleschi V 2010 Calibration-Free Laser-Induced Breakdown Spectroscopy: State of the art *Spectrochim. Acta - Part B At. Spectrosc.* **65** 1–14

[9] Cristoforetti G, De Giacomo A, Dell'Aglio M, Legnaioli S, Tognoni E, Palleschi V and Omenetto N 2010 Local Thermodynamic Equilibrium in Laser-Induced Breakdown Spectroscopy: Beyond

the McWhirter criterion *Spectrochim. Acta - Part B At. Spectrosc.* **65** 86–95

[10] Wang P, Jacob W, Gao L, Dürbeck T and Schwarz-Selinger T 2013 Comparing deuterium retention in tungsten films measured by temperature programmed desorption and nuclear reaction analysis *Nucl. Instruments Methods Phys. Res. Sect. B Beam Interact. with Mater. Atoms* **300** 54–61

[11] Piip K, Paris P, Hakola A, Bystrov K, De Temmerman G, Aints M, Jõgi I, Kozlova J, Laan M, Likonen J, Lissovski A and Mändar H 2014 Influence of He/D2 plasma fluxes on the morphology and crystallinity of tungsten coatings *Phys. Scr.* **89**

[12] Piip K, De Temmerman G, Van Der Meiden H J, Lissovski A, Karhunen J, Aints M, Hakola A, Paris P, Laan M, Likonen J, Jõgi I, Kozlova J and Mändar H 2015 LIBS analysis of tungsten coatings exposed to Magnum PSI ELM-like plasma *J. Nucl. Mater.* **463**

[13] Piip K, van der Meiden H J, Hämarik L, Karhunen J, Hakola A, Laan M, Paris P, Aints M, Likonen J, Bystrov K, Kozlova J, Založnik A, Kelemen M and Markelj S 2017 LIBS detection of erosion/deposition and deuterium retention resulting from exposure to Pilot-PSI plasmas *J. Nucl. Mater.* **489** 129–36

[14] Kreter A, Nishijima D, Doerner R P, Freisinger M, Linsmeier C, Martynova Y, Möller S, Rasinski M, Reinhart M, Terra A, Torikai Y and Unterberg B 2019 Influence of plasma impurities on the fuel retention in tungsten *Nucl. Fusion* **59**

[15] Takamura S, Aota T, Uesugi Y, Kikuchi Y, Maenaka S and Fujita K 2019 Effects of nitrogen-seeded deuterium plasma on tungsten surfaces *Nucl. Fusion* **59**

[16] Uccello A, Ghezzi F, Laguardia L, Caniello R, Dellasega D, dell'Era F, Della Torre D, Donnini R, Granucci G, Mesto E, Minelli D, Passoni M, Pedroni M, Pezzoli A and Ricci D 2020 Effects of a nitrogen seeded plasma on nanostructured tungsten films having fusion-relevant features *Nucl. Mater. Energy* **25** 100808

[17] Ogorodnikova O V., Sugiyama K, Markin A, Gasparyan Y, Efimov V, Manhard A and Balden M 2011 Effect of nitrogen seeding into deuterium plasma on deuterium retention in tungsten *Phys. Scr. T* **T145**

[18] Lee H T, De Temmerman G, Gao L, Schwarz-Selinger T, Meisl G, Höschen T and Ueda Y 2015 Deuterium retention in tungsten exposed to mixed D + N plasma at divertor relevant fluxes in Magnum-PSI *J. Nucl. Mater.* **463** 974–8

[19] Grigore E, Gherendi M, Hernandez C, Desgranges C and Firdaouss M 2016 Tungsten coatings for application in WEST project *Nucl. Mater. Energy* **9** 137–40

[20] Roth J and Schmid K 2011 Hydrogen in tungsten as plasma-facing material *Phys. Scr. T* **T145**

[21] Van Der Meiden H J, Van Den Berg M A, Brons S, Ding H, Van Eck H J N, 'T Hoen M H J, Karhunen J, De Kruif T M, Laan M, Li C, Lissovski A, Morgan T W, Paris P, Piip K, Van De Pol M J, Scannell R, Scholten J, Smeets P H M, Spork C, Zeijlmans Van Emmichoven P A, Zoomers R and De Temmerman G 2013 Laser-based diagnostics applications for plasma-surface interaction studies *J. Instrum.* **8**

[22] Paris P, Jõgi I, Piip K, Passoni M, Dellasega D, Grigore E, Arnoldbik W M and van der Meiden H 2021 In-situ LIBS and NRA deuterium retention study in porous W-O and compact W coatings loaded by Magnum-PSI *Fusion Eng. Des.* **168** 23–7

[23] Costin C, Anita V, Popa G, Scholten J and De Temmerman G 2016 Tailoring the charged particle fluxes across the target surface of Magnum-PSI *Plasma Sources Sci. Technol.* **25**